

The research programme of the Laboratory of Radiation Biology (LRB) determined by the 1st priority theme 04-9-1015-96/2008 «Radiation and Radiobiological Investigations at the JINR Basic Facilities and in the Environment» was finished in 2008 and concentrated on the following main directions: fundamental radiobiological and radiation genetic research with heavy charged particle beams, investigation of molecular photo- and radiobiological processes in eye structures, molecular dynamics research, and radiation re-

search and radiation protection at the JINR basic facilities and in the environment. Special attention was paid to the participation of young researchers, students, and postgraduates in the LRB's current events and in conferences and seminars where the LRB took part. Beginning with 2009, the LRB will continue its research in the framework of the new 1st priority theme 04-9-1077-2009/2011 «Research of Biological Action of Heavy Charged Particles with Different Energy».

RADIOBIOLOGICAL AND RADIATION GENETIC RESEARCH

Complex research on the biological action of ionizing radiation with different physical characteristics has been continued. Regularities of the induction and repair of DNA lesions in peripheral human blood lymphocytes under the action of radiation in a wide range of linear energy transfer (LET) have been studied. Using the DNA comet techniques, regularities of the formation of DNA single-strand breaks (SSB) and double-strand breaks (DSB) in human lymphocytes under irradiation by ^{60}Co gamma rays and accelerated lithium and boron ions with energy of 40 MeV/nucleon have been examined. It has been found that the DNA SSB and DSB yield grows linearly with the dose, the SSB formation efficiency being much higher (Fig. 1).

The kinetics of the DNA SSB and DSB repair in lymphocytes has been studied during a period of up to 96 h following irradiation by gamma rays. It has been found that the DNA SSB and DSB yield decreases exponentially in the post-irradiation period and in 24 h reaches the reference values (Fig. 2). This level holds during a further storage of up to 96 h. A modifying influence has been studied of DNA repair inhibitors — *cytosine arabinoside* (Ara C) and *hydroxyurea* (HU) — on the induction and repair of DNA DSB in human lymphocytes upon irradiation by ^{60}Co gamma rays and accelerated boron ions. It has been found that under the influence of the inhibitors, the number of DNA DSB increases, which seems to be connected with active accumulation of enzymatic DNA DSB. Without Ara-C and HU, the DNA DSB repair is fully completed in 4–6 h.

Regularities have been studied in the induction of apoptosis in human lymphocytes by ^{60}Co gamma rays in different time after irradiation (Fig. 3). Variability has been found in the results for donors of different ages — from 21 to 62 years. It is shown that the temperature conditions (0°C and room temperature) do not influence the apoptotic cell death frequency under gamma-irradiation. Comparative experiments have been performed on newly extracted and frozen (i.e., kept 7 days at -70°C in 10% DMSO after extraction) lymphocytes. It is shown that in both cases the frequency of apoptotic cell formation is practically the same during the post-irradiation period of 0–24 h and is significantly different in further incubation [10].

Regularities of the induction of different mutation-related lesions by ionizing radiation in *saccharomycete* yeasts have been studied [5, 6, 8]. An analysis of the loss of chromosome IV — one of the biggest chromosomes of yeasts (1554 TPN) — under the action of UV and gamma rays in disomic strains shows that chromosome IV is unstable and is lost more frequently than earlier studied chromosome VII. For example, with the absorbed radiation dose of 100 J/m^2 and cell survivability of $\sim 1\%$, the chromosome loss frequency is $20 \cdot 10^{-3}$, while for a gamma ray dose of 100 Gy and survivability of 10%, it is $4 \cdot 10^{-3}$. A linear dependence of the chromosome loss induction on the dose is observed. The spontaneous chromosome loss frequency is $4 \cdot 10^{-4}$.

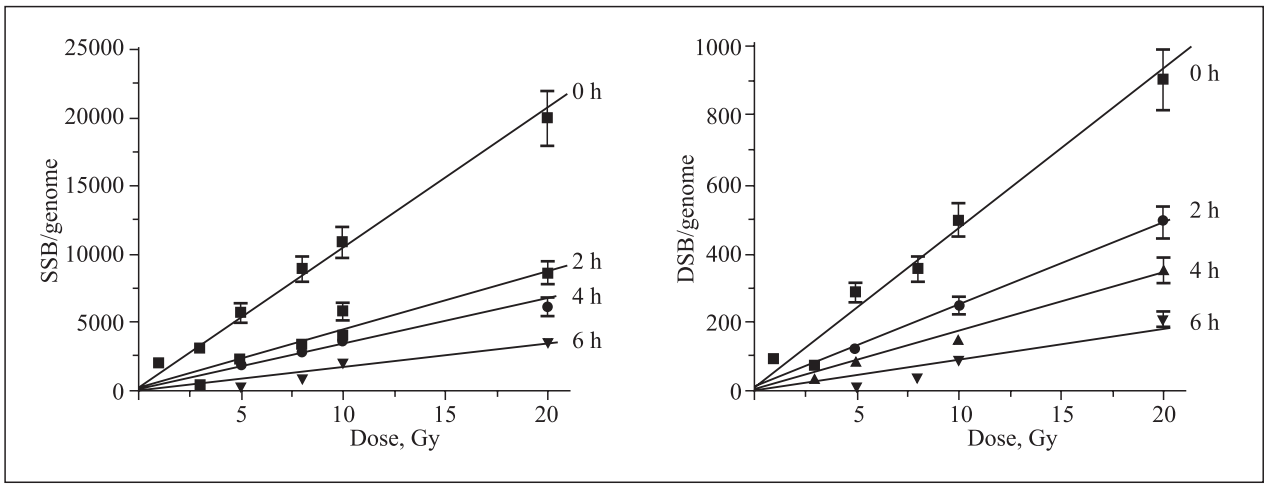


Fig. 1. Dose dependences of the DNA SSB and DSB yield in different time (2, 4, and 6 h) after γ -irradiation

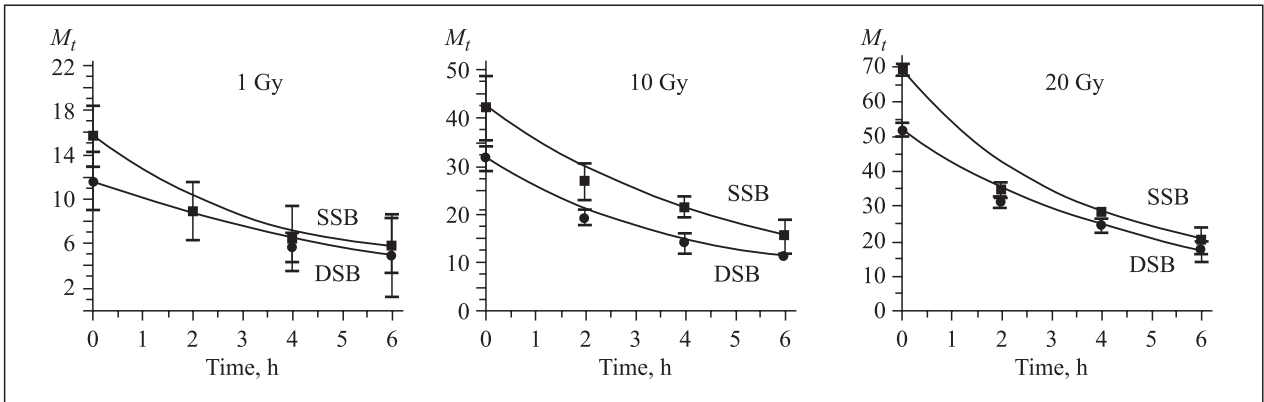


Fig. 2. Kinetics of the DNA SSB and DSB repair after γ -irradiation with doses of 1, 10, and 20 Gy

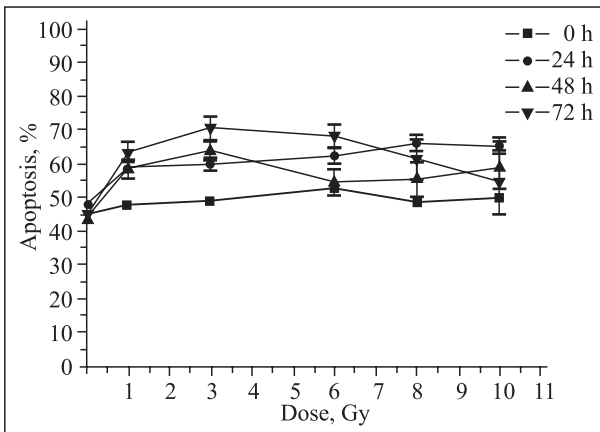


Fig. 3. Dose dependence of the frequency of apoptotic cell formation in different time after γ -irradiation

The phenomenon of adaptive response (AR) in peripheral human blood lymphocytes has been studied. The main aim of the research was to find out possible

reasons for individual variability in the AR of different donors' lymphocytes. A cytogenetic analysis of chromosome aberrations in human blood upon irradiation by 145 MeV and Bragg-peak protons at the therapeutic proton beam of the JINR phasotron [3] has been performed. It is shown that the Bragg-peak protons are 1.25 times more efficient in the dose range of 1–4 Gy. A comparative analysis has been performed of the individual radiosensitivity of chromosomes 2, 8, and 14 of human lymphocytes to irradiation by charged particles with different LET. At JINR accelerator, healthy donors' whole blood samples were irradiated by accelerated protons and carbon, lithium, and boron ions with the doses of 3, 3.5, and 4 Gy. At the sample locations, the particle energy and LET were, respectively, as follows: 170 MeV and ≈ 0.5 keV/ μ m for protons; 480 MeV and ≈ 10.6 keV/ μ m for ^{12}C ; 30 MeV/nucleon and ≈ 20 keV/ μ m for ^7Li ; 32 MeV/nucleon and ≈ 55 keV/ μ m for ^{11}B . A series of experiments were completed at GSI (Gesellschaft für Schwerionenforschung, Darmstadt, Germany) which were performed in collaboration with its Department of Biophysics. The

experiments were aimed at studying chromosome aberrations and proliferative activity in human peripheral blood lymphocytes under the action of accelerated iron ions of different energies and LET [4, 12–14, 17]. To study the human lymphocyte cell response to radiation with different LET, unstimulated isolated lymphocytes were irradiated by accelerated iron ions with energies of 1000 and 200 MeV/nucleon (with a LET of 155 and 335 keV/ μm , respectively) and X-rays. Chromosome aberrations and cycle cell progression were analyzed in the first post-irradiation metaphase cycles 48, 60, 72, and 84 h after irradiation, so practically all dividing cells were included in the analysis. It is shown that after X-ray irradiation, the numbers of aberrations and aberrant cells do not depend on fixing periods. A significant growth in these parameters (two times between 48 and 84 h after irradiation) was observed after irradiation with iron ions with a LET of 155 keV/ μm and 8–10 times after irradiation with iron ions with a LET of 335 keV/ μm . This reflects a time delay in the division of the most heavily damaged cells, which has a pronounced dependence on LET. The effect was yet stronger as LET was higher and ion energy was

lower. The coefficients of the relative biological effectiveness (RBE) concerning the chromosome aberration yield varied from 3.0 after 48 h to 7.0 after 84 h of cultivation upon irradiation with iron ions with a LET of 155 keV/ μm , and, respectively, from 0.5 to 3.0 upon irradiation with iron ions with a LET of 335 keV/ μm .

A mathematical model has been developed of the UV irradiation-induced mutation process in the bacterium *Escherichia coli*. It is the first time that on the basis of experimental data, the molecular process has been described that connects the initial stages of the formation of primary DNA lesions with their fixing as mutations [1, 2]. The proposed model concepts have allowed the dynamics of the dimerized products of the *umuD* gene and the main regulatory complexes of the SOS repair system of *Escherichia coli* cells, which has not been studied before, to be predicted.

The developed model concepts have for the first time allowed the dynamics of the dimerized products of the *umuD* gene (Fig. 4) and two regulatory complexes of the SOS system — UmuD₂C and UmuDD'C (Fig. 5) — to be predicted.

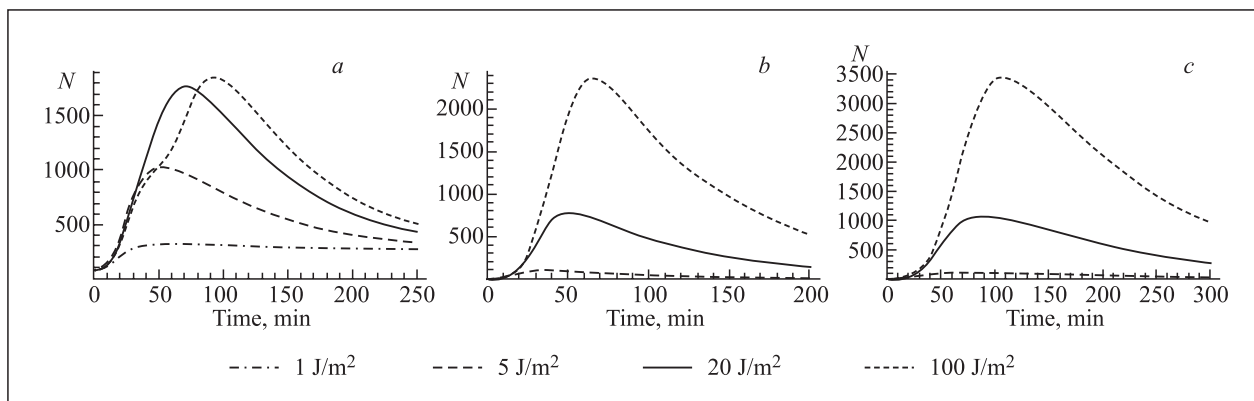


Fig. 4. Numerical calculation of the concentration dynamics of the dimerized protein products of the *umuD* gene for the proteins UmuD₂ (a), UmuD'₂ (b), and UmuDD' (c)

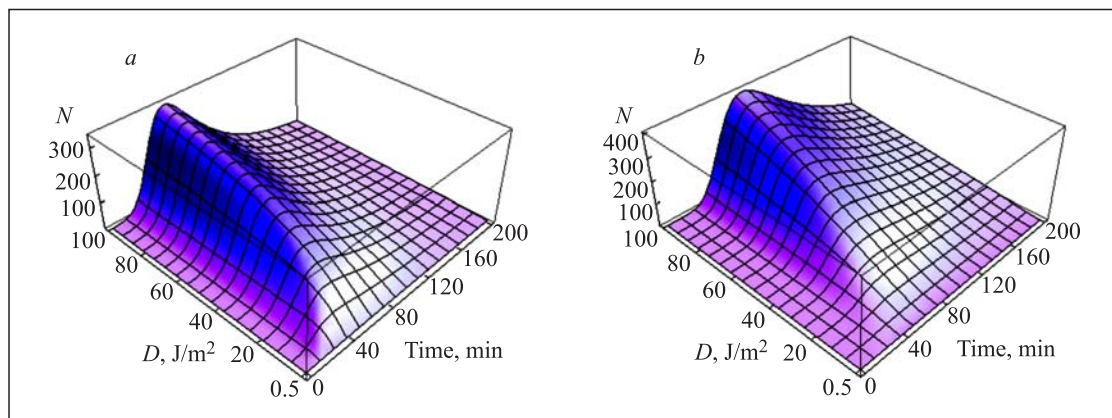


Fig. 5. Numerical calculation of the concentration dynamics of the protein complexes UmuD₂C (a) and UmuDD'C (b)

Research has been continued on the regularities of apoptotic response induced in mouse retina cells by methylnitrosourea (MNU) and ionizing radiation [7]. The research is aimed at further studying *in vivo* the signaling pathway connecting the primary DNA lesions induced by MNU, gamma rays, and protons with mouse retina cell death. It has been found that immediately (no later than in 2 h) upon introducing MNU, primary DNA lesions are observed as apurinic or apyrimidinic sites (AS), which emerge as a result of the activation of N-glycosylases in the mechanism of the excision repair of methylated bases. Repair of lesions completes 6 h after exposure leaves about 50% of initial lesions unrepaired, which remain up to 72 h (Fig. 6). Along with this process, the number of DNA double-strand breaks in retina cells grows monotonically. These breaks are an indicator of the apoptotic degradation of the genome. Their number reaches the maximum in 48 h. Apoptosis has been confirmed by the analysis of the morphologic changes in the external nuclear layer. But the expression of P53 — a universally recognized regulator in apoptotic signaling in cells — has not been observed. The retina responses to gamma rays (14 Gy) and 170 MeV protons (14 and 25 Gy) were similar: the DNA single- and double-strand breaks induced by these irradiations were efficiently and fully repaired within 6 h. Also, in response to proton irradiation, ATM and P53 expression was observed in retina cells in 2–4 h and ≥ 12 h, respectively. No convincing apoptosis indicators have been observed after irradiation. Nicotinamide (Nam) — a PARP-mediated inhibitor of break repair — slowed down DNA repair in the retina after introducing MNU. But the portion of unrepaired lesions was in this case the same as without introducing MNU — 50%. In this process, apoptosis was fully blocked according to the tissue and cell morphology criteria. A conclusion has been drawn that the retina stability against apoptotic signals is accounted for by the efficient repair of radiation lesions in the transcribable part of the genome of the differentiated cells.

In experiments on C57Black \times CBA F1 male mice, research has been continued on the influence of a combination of a single exposure to gamma rays with subsequent daily UV irradiation on a cataract formation. It is shown that on the 6th month after the experiment beginning, weak cortical opacities (1–2 points) develop in all the experimental groups' crystalline lenses. Some of the gamma-irradiated mice also developed posterior polar opacities.

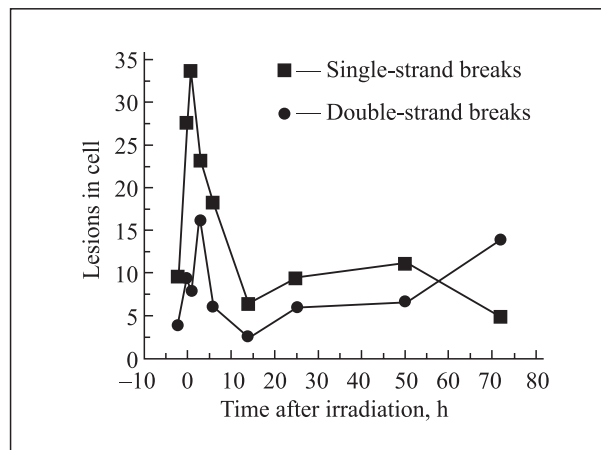


Fig. 6. Dynamics of the content of DNA single- and double-strand breaks in mouse retina cells after γ -irradiation (DNA-comet method)

Statistically significant difference in the degree of the crystalline lens damage has been found between the mice that got a dose of 2 Gy and the mice that got a combination of a dose of 4 Gy and UV irradiation ($p = 0.015$, the Mann–Whitney test).

On the 9th month, the opacity density significantly increased, with the difference in the degree of the crystalline lens damage between different groups being somewhat reduced due to the natural ageing of the mice. In the gamma-irradiated group, the flattening of the epithelium cells and defragmentation of their nuclei have been observed (Fig. 7).

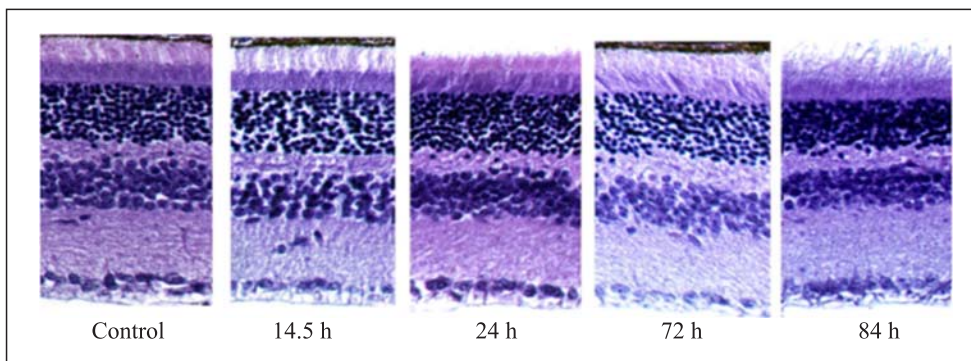


Fig. 7. Microphotographs of histological cuts of a mouse retina before and after γ -irradiation

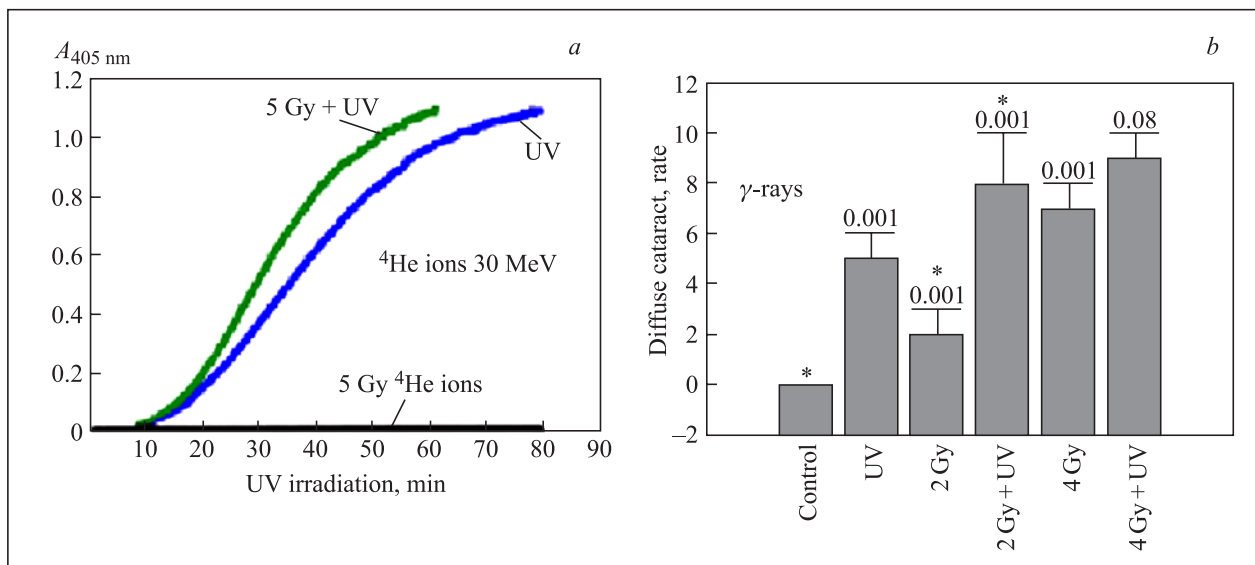


Fig. 8. Radiation lesions in the eye lens crystallines (a) and cataract induction in mice (b) under the combined effect of ionizing and UV irradiation

The cell monolayer density was lower for a dose of 2 Gy and much lower for a dose of 4 Gy. On the epithelium layer surface, separate desquamated cells have been observed. Under the action of two damaging factors — gamma and UV radiation — a combination of the mentioned lesions has been observed, but in this case, there were areas of cubic epithelium transforming into flat one with the formation of two cell layers and areas of capsule detachment from the crystalline lens cell mass. In the case of a combination of a dose of 4 Gy and UV

irradiation, a substantial decrease in the epithelium cell density has been observed along with the emergence of cells with large nuclei and sites of epithelium cells transforming into fibroblast-like cells, which formed multi-layer structures. But no significant difference has been found between the groups (the Mann-Whitney nonparametric test). Thus, UV radiation, gamma radiation, and their combination induce changes in the morphology of cataractal crystalline lens cells, but they are not specific to each of the exposures (Fig. 8).

COMPUTER MOLECULAR MODELING OF BIOPHYSICAL SYSTEMS

Using computer modeling techniques, a comparative study has been performed of the molecular dynamics of rhodopsin containing a chromophore group (11-*cis*-retinal) and free opsin [9, 11, 15]. It is shown that incorporation of a chromophore group into the chromophore center of the opsin has a significant influence on the nearest protein surroundings of chromophore and on the conformation state of the cytoplasmatic domain, and has practically no influence on the conformation state of the intra-disk domain. On the basis of modeling results, a possible intra-molecular mechanism of keeping rhodopsin inactive as a G-protein-binding receptor has been considered. A series of works have been carried out to model cyclin-dependent protein kinases (CDK) with an ATP complex. To analyze the structure changes to which a replacement of CDC28-G20S leads, the crystalline structure of human kinase CDK2 was used. According to the molecular dynamic modeling results, the structures of the nonmutant and mutant (including the replacement of G16S-CDK2 corresponding

to the yeast G20S-CDC28) CDK2 complexes notably differ from each other. It is the sites playing the key role in the kinase functioning (for example, the G- and T-loops) where differences between the structural conformations are most apparent.

Molecular dynamics simulations on visual pigment rhodopsin with E181K mutation which is associated with retinitis pigmentosa are performed. Autosomal dominant retinitis pigmentosa leads to the photoreceptor cell death and retina degeneration. Approximately 25% of this pathology is associated with the rhodopsin gene mutation RP4(RHO)/Rhodopsin(3q). The amino acid substitution in the chromophore center during rhodopsin biosynthesis leads to the most distinctive clinical pathology of this inherited disease. The consequence of mutations like these is protein misfolding. As a result, formation of a stable Schiff base linkage between the 11-*cis*-retinal chromophore and amino acid residue Lys296 is impossible. Using molecular simulation technique, the process of 11-*cis*-retinal chromophore em-

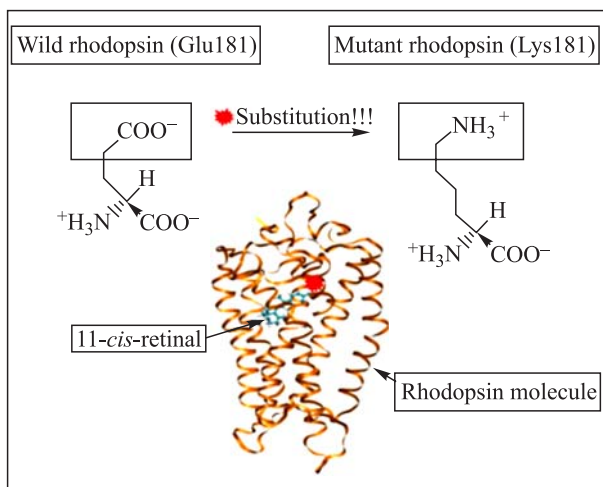


Fig. 9. Mutant form of rhodopsin E181K

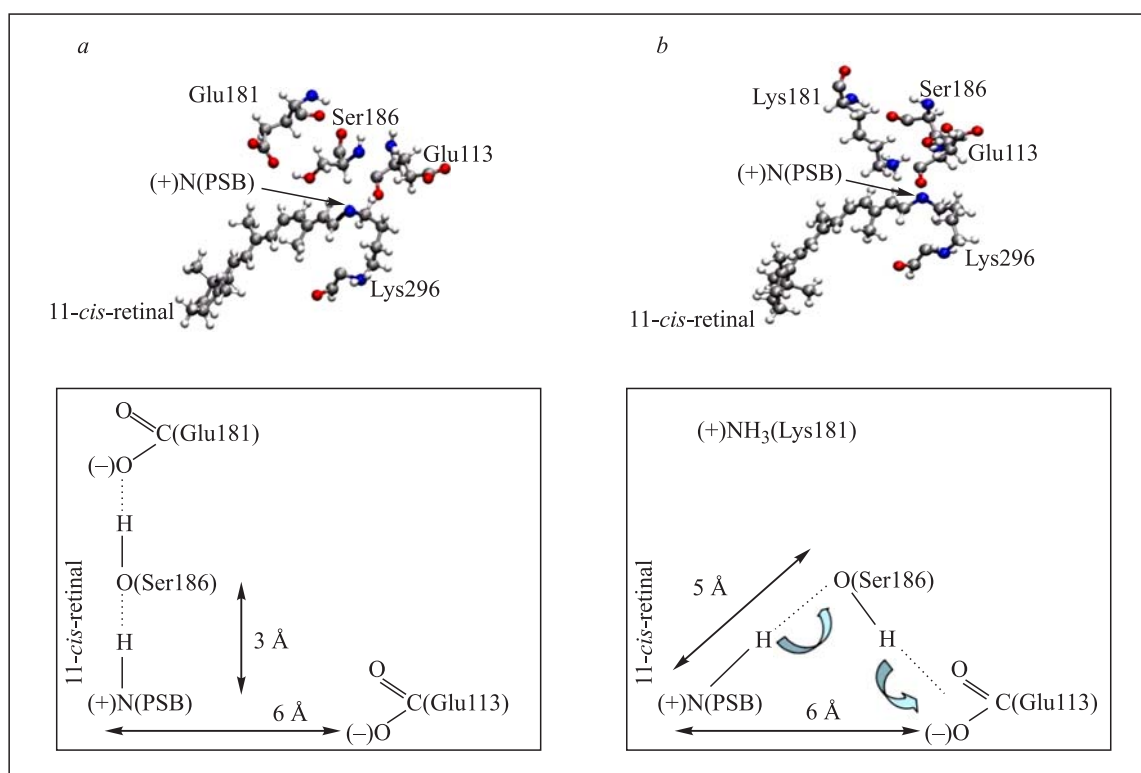


Fig. 10. MD analysis of the native (a) and mutant (b) E181K forms of rhodopsin protein

In [16, 18] a comparative analysis of 3D simulation of different allele forms of human kinase CDK2 has been performed. The crystal structures of the human CDK2/cyclin A complex have been solved. We simulated the wild-type structure and mutant allele with a single substitution of glycine with serine in position 16 (G16S) in conservative G-rich loop. It was shown that this substitution causes a serious modification in protein structure. In yeast such changes of homologous kinase CDC28 have serious pleiotropic biological effects. To investigate the significance of

bedding into the chromophore center of opsin mutant form has been investigated. The comparative analysis of amino acid residues arrangement in the opsin chromophore center and its interaction with 11-*cis*-retinal as in the wild (native) as in the mutant opsins has been carried out. It was shown that there is no normal embedding of the 11-*cis*-retinal into the chromophore center of the opsin mutant form (Fig. 9). As a result, the impairment of conformation state of the opsin molecule takes place both in the chromophore center and in the cytoplasmic domain. A stable covalent linkage of the 11-*cis*-retinal with the protein part of rhodopsin molecule is not formed, and the active site in the cytoplasmic domain of the protein, responsible for binding the G-protein (so-called transducin) is also not blocked. Based on the molecular simulation data, the problem related to retinitis pigmentosa pathogenesis is discussed (Fig. 10).

the observed structural modifications we studied the structure of another mutant allele R274Q which in yeast has not biological effects at permissive temperature. A comparison of simulated CDK2 structures of three alleles shows that root mean square deviation of the kinase and kinase + cyclin do not change in the last allele of kinase; although the structures of the T- and G-loops were modified. These results confirm the correlation between the observed changes of the kinase structure and biological effect (Fig. 11).

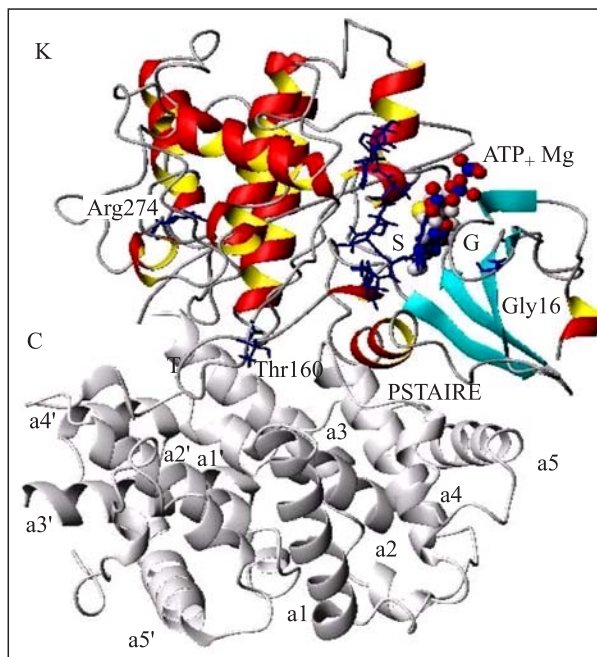


Fig. 11. A ribbon structure of human protein kinase model CDK2 (entry file 1QMZ from PDB database). The protein complex consists of a kinase (K) and a cyclin A (C) parts, etc.

The MD simulation code optimization and adjustment to different communication architectures for computational chemistry and nanotechnology problems are

fulfilled at the JINR computing farm in collaboration with Daresbury Laboratory (UK), RIKEN, and Keio University (Japan).

RADIATION RESEARCH

The work connected with the NICA radiation system design was continued in 2008. The crucial problem determining the radiation situation around the NICA complex is the problem of the «skyshine» neutron dose on board of a spacecraft in the control area where the annual total dose cannot exceed the dose limit of 1 mSv for population. All radiation shields at the NICA radiation sources must be designed taking into account this criterion. The most powerful radiation sources at the complex will be the Nuclotron, collider ring, and beam stoppers in the case of accelerating uranium nuclei to an energy of 4.5 GeV/n. The different versions of the booster and Nuclotron, collider ring shields were simulated by the GEANT4 code for various NICA operation modes [19]. The preliminary verification of the universal MC codes FLUKA, SHIELD and GEANT4 for radiation transport in matter calculation was done as well on the basis of experimental data on the neutron yields from a thick iron target irradiated by ^{238}U nuclei with energies up to 1 GeV/n [20]. The technical draft proposal for the radiation shielding design was prepared.

The investigations connected with the development, computer modeling, and physical calibration of the Russian neutron detectors DAN (Dynamic Albedo Neu-

trons) and LEND (Lunar Exploration Neutron Detector) designed for the Mars and Moon surface research by nuclear physics methods were continued in collaboration with the FLNP and the Institute of Space Research (Moscow) [21, 22]. The setup works for the LEND are now practically completed before the spacecraft launch. The DAN calibration was done with pseudo-environmental tests and showed the high sensitivity of the detector for the underground water (ice) exploration by the NACA rover (Mars Science Laboratory).

Work within the framework of the project «Development of New Protection Materials and Thermo Luminescent Detectors for Radiation Safety Measures» of the complex long-term cooperation program between Russia and India was continued. The experiments were performed at a 150 MeV proton beam on studying the properties of several tens of thermo luminescent phosphors fabricated in India using nano- and microtechnologies. Other experiments on studying the properties of protection materials fabricated in India were carried out as well.

The simulation of the ridge filter designed for the carbon therapy installation was done using the MC code.

The 3rd international workshop «Molecular Simulation Studies in Material and Biological Sciences» (MSSMBS'08) was held on 10–12 September at JINR. Scientists from research centers and universities of Japan and Europe, leading research centres of Russia (Institute of Bioorganic Chemistry, Institute of Biochemical Physics, Institute of Mathematical Problems of Biology, and MSU) as well as from the LRB and LIT attended the workshop. The workshop scientific programme reflected the current status and prospects of computer molecular simulation in modern science. The MSSMBS-2008 scientific programme covered the following topics: protein modeling, drug design, simulation of liquids and polymer systems, simulation of radiation-induced lesions and mutations, quantum biophysics, and parallel computing for chemical physics and biomolecular studies.

The education process at the chair «Biophysics» of the International University «Dubna» was continued. 76 students in sum are studying now on specialty — «Radiation Protection of People and Environment» and 17 new students were admitted in 2008 to the chair. The 4th graduation of 7 students took place in 2008.

REFERENCES

1. *Belov O. V., Krasavin E. A., Parkhomenko A. Yu.* Mathematical Model of the Ultraviolet-Induced Mutation Process in the Bacterium *Escherichia coli*. JINR P19-2008-105. Dubna, 2008 (in Russian).
2. *Belov O. V.* Time Dependence of the Inducing Signal of the SOS System of the Bacterium *E. coli* under Ultraviolet Irradiation // Part. Nucl., Lett. 2007. V. 4, No. 6(142). P. 867–874 (in Russian).
3. *Zaytseva E. M.* Study of Chromosome Aberrations in Human Cells Irradiated by a Therapeutic Proton Beam // Proc. of VII Conf. of Young Scientists, Specialists, and Students Timed to the Cosmonautics Day and 45th Anniversary of the Institute of Medical and Biological Problems of the Russian Academy of Sciences, Moscow, April 2008. P. 23 (in Russian).
4. *Koshlan I. V., Koshlan N. A.* Chromosome Instability of HPRT Mutants Induced by Gamma Quanta and Accelerated Lithium (^7Li) Ions // Ibid. P. 32 (in Russian).
5. *Koltovaya N. A. et al.* Interaction between the Checkpoint Genes *RAD9*, *RAD17*, *RAD24*, and *RAD53* in Evaluating the Sensitivity of the Yeasts *Saccharomyces cerevisiae* to Ionizing Radiation // Genetics. 2008. V. 44, No. 6. P. 659–668 (in Russian).
6. *Koltovaya N. A. et al.* Interaction between the Checkpoint Genes *RAD9*, *RAD17*, *RAD24*, and *RAD53* with the Genes *SRM5/CDC28*, *SRM8/NET1*, and *SRM12/HF11* in Evaluating the Sensitivity of the Yeasts *Saccharomyces cerevisiae* to Ionizing Radiation // Ibid. No. 8. P. 909–918 (in Russian).
7. *Loginova M. Yu. et al.* Retina Radioresistance: under the Action of Gamma Radiation, DNA Breaks Form and the Protein P53 Content Increases in Mouse Retina, Which Is Accompanied by DNA Repair and Absence of Cell Apoptosis // Rad. Biology and Radioecology. 2008. V. 48, No. 6. P. 698–704 (in Russian).
8. *Stepanova A. N., Koltovaya N. A.* UV-Induced Loss of DNA Fragments in the Yeasts *Saccharomyces cerevisiae*. JINR Commun. P19-2008-97. Dubna, 2008. P. 1–5 (in Russian).
9. *Feldman T. B., Kholmurodov Kh. T., Ostrovsky M. A.* Computer Modeling of the Molecular Physiology of the Visual Pigment Rhodopsin // Part. Nucl., Lett. 2008. No. 1. P. 25–49 (in Russian).
10. *Chausov V. N. et al.* Regularities of the Induction and Repair of DNA Double-Strand Breaks in Human Lymphocytes under the Action of Accelerated Heavy Ions with Different Energies // Rad. Biology and Radioecology. 2009. V. 49, No. 7. P. 73–77 (in Russian).
11. *Kholmurodov Kh. T., Feldman T. B., Ostrovsky M. A.* Molecular Modeling of the Visual Pigment Rhodopsin with the Point Mutation E181K Related to the Pigment Retinitis Pathogenesis // Ophthalmology. 2008. No. 1. P. 39–43 (in Russian).
12. *Hartel C. et al.* Chromosome Aberrations in Lymphocytes of Prostate Cancer Patients Treated with IMRT and Carbon Ions // The 36th Annual Meeting of the Eur. Rad. Research Society Tours, France, Sept., 2008. P. 1–4.
13. *Hartel C. et al.* Chromosome Aberrations in Blood Lymphocytes of Prostate Cancer Patients // GSI Sci. Report 2008. GSI-2008-1.
14. *Lee R. et al.* Cytogenetic Damage in Human Blood Lymphocytes Exposed *in vitro* and *in vivo* to Space-Relevant HZE-Particles // The 37th COSPAR Assembly, Montréal, July 2008. P. 13–20.
15. *Kholmurodov Kh. T., Feldman T. B., Ostrovsky M. A.* Interaction of Chromophore, 11-*cis*-retinal, with Amino Acid Residues of the Visual Pigment Rhodopsin in the Region of Protonated Schiff Base: a Molecular Dynamics Study // Rus. Chem. Bull. Intern. Edition. 2008. V. 56, No. 1. P. 20–27.
16. *Kholmurodov Kh. T., Koltovaya N. A.* Comparison of 3D Simulated of Different Allele Forms of Human Kinase CDK2 // The 3rd Intern. Workshop MSSMBS'2008, Dubna, Sept. 10–12, 2008. P. 29–30.
17. *Zahnreich S. et al.* Genetic Instability and Telomere Shortening in Normal Human Fibroblasts after Irradiation with X-Rays // GSI Sci. Report 2008. GSI-2008-1.
18. *Koltovaya N. A. et al.* Sequencing Analysis of Mutant Allele CDC28-srm of Protein Kinase CDC28 and Molecular Dynamics Study of Glycine-Rich Loop in Wild Type and Mutant Allele G16S of CDK2 as Model // Acta Physi-

- ologica Congress. J. of Federation of Eur. Physiol. Soc. 2008. Abstr. No.037P.
19. *Timoshenko G. et al.* Monte-Carlo Simulations for Estimation of the Radiation Environment around the Modernized Nuclotron // Proc. of RUPAC2008, Zvenigorod, Russia, Sept. 28–Oct. 3, 2008; <http://accelconf.web.cern.ch/AccelConf/r08/papers/FRBAU02.pdf>
 20. *Beskrovnaia L. et al.* Verification of Monte-Carlo Transport Codes FLUKA, GEANT4 and SHIELD for Radiation Protection Purposes at Relativistic Heavy Ion Accelerators // Nucl. Instr. Meth. B. 2008. V.266. P.4058–4060.
 21. *Litvak M.L. et al.* The Dynamic Albedo of Neutrons (DAN) Experiment for NASA's 2009 Mars Science Laboratory // Astrobiology. 2008. V. 8, Iss. 3. P. 605–612.
 22. *Mitrofanov I.G. et al.* Experiment LEND of the NASA Lunar Reconnaissance Orbiter for High-Resolution Mapping of Neutron Emission of the Moon // Ibid. Iss. 4. P. 793–804.